# Role of humic acid in enhancing dissolved air flotation for the removal of TiO2 nanoparticles

Ming Zhang, Jean-Luc Trompette, Pascal Guiraud

# Role of Humic Acid in Enhancing Dissolved Air Flotation for the Removal of $TiO_2$ Nanoparticles

Ming Zhang,[†,§] Jean-Luc Trompette,[‡] and Pascal Guiraud*[,†]

[†]LISBP, Université de Toulouse, CNRS, INRA, INSA, 31077 Toulouse, France
[‡]LGC, CNRS, INPT, UPS, 31432 Toulouse, France

DOI: 10.1021/acs.iecr.6b04572

**ABSTRACT:** The particle separation efficiency by flotation sharply decreases or even completely fails when the diameter of dispersed particles falls into the nanoscale. In the present laboratory work, humic acid was used to enhance the removal of $TiO_2$ nanoparticles from suspension in a chemical coagulant-free dissolved air flotation process. Without humic acid, merely 63.8% of $TiO_2$ nanoparticles were removed. For the humic acid-assisted dissolved air flotation, the pH of humic acid solution significantly influenced the removal efficiency: more than 90% of nanoparticles could be separated when the pH of the humic acid stock solution was acidic; however, the basic solutions resulted in rather poor performance. In the acidic solution, the fiberlike humic acid might form colloids through the attraction between hydrophobic moieties. They possibly acted as a fishnet and trapped nanoparticles, leading to the great measured bubble−particle attachment efficiency. In all the effluents, a low residual dissolved organic carbon was observed, revealing a good participation of humic acid in flotation. Moreover, a higher air-to-solid ratio could improve the nanoparticle elimination by offering a larger surface area of air bubbles. The fractal dimension of flotation flocs demonstrated that the aggregates with compact structure took greater advantage in the flotation separation of nanoparticles.

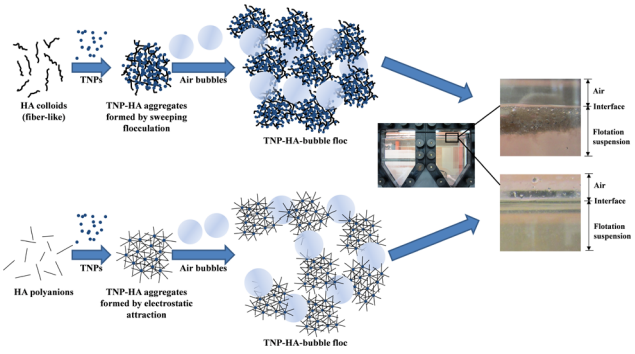


## 1. INTRODUCTION

Titanium dioxide ($TiO_2$), frequently used as a white pigment, is incorporated into a wide range of industrial products like paints, papers, lacquers, and ceramics. It becomes transparent at the nanoscale, being able to absorb and reflect ultraviolet light. $TiO_2$ nanoparticles (TNPs) are abundantly produced and widely applied because of their high stability and anticorrosion and photocatalysis properties.[1] Consequently, it is inevitable that those products and byproducts enter the aquatic environment.[2] Release of TNPs may come from point sources, such as industrial effluents, or from nonpoint sources, such as wet deposition from atmosphere, stormwater runoff, and attrition of products containing TNPs.[3] For instance, the runoff emanating from rainwash of building surfaces may contain a high amount of TNPs. The fate of TNPs in the ecosystem and their effects on the human health are of growing concerns. Their possible major entries into cells are endocytotic routes.[2] Compared with bulk and fine $TiO_2$ particles, the TNPs are more likely to generate damaging reactive oxygen species (ROS).[4] An excessive and sustained increase in ROS has been implicated in the pathogenesis of cancer, diabetes mellitus, and other diseases.[5] Hepatic injury, renal lesion, and myocardial damage may result from the retention of TNPs in the liver, kidneys, and other tissues.[6] These health and eco-environmental risks demonstrate a strong need for the development of effective treatment processes to remove TNPs from wastewaters.

Flotation has a great potential in the removal of nanoparticles (NPs) and submicrometer particles from wastewaters. Techniques such as carrier flotation and agglomerate flotation have been suggested as ways of increasing flotation rates of colloids and ultrafines.[7,8] The collision dynamics is regarded as one of the most crucial factors deciding the collection efficiency of particles by flotation.[9,10] NPs with diameter less than 100 nm undergo Brownian diffusion, which is considered as the principal NP−bubble collision mechanism. When particles are large enough to be unaffected by Brownian motion, i.e., greater than some micrometers, the interception mechanism plays a dominant role; the bubble−particle collision efficiency rises with the increase of size ratio between particles and bubbles.[11,12]

In order to achieve the high NP removal, two important approaches for improving the capture efficiency of NPs by flotation can be determined: (i) reducing the bubble size to gain a high specific surface area of bubbles as well as to reinforce the Brownian diffusion mechanism and/or (ii)

increasing the particle−particle interaction to form the nanoparticle aggregates and thus to facilitate the interception mechanism.[13] For the former, dissolved air flotation (DAF) has been extensively adopted and was obviously chosen in this study. Tiny bubbles with the diameter of 40−80 $\mu$m are produced in the DAF process by releasing the pressurized water (400−600 kPa) in the contact zone.[14] For the latter, coagulants and/or flocculants are introduced as flotation-assisting reagents so that the coagulation of particles and the heterocoagulation of bubble−particle can be beneficial through charge neutralization, sweep flocculation, and so forth.[15] Lien and Liu tested the treatment of chemical mechanical polishing (one of its main components is silica NP) effluents by DAF.[16] The effective removal of particles from wastewater was found when using the cationic surfactant cetyltrimethylammonium bromide as collector. Liu et al. also found that silica NPs could be well removed by DAF combined with the surfactant aided coagulation process.[17] However, apart from surfactants and traditional coagulants/flocculants, novel and environmentally friendly flotation-assisting reagents are still required. With their help, NPs are expected to be effectively and efficiently removed, but concomitantly, fewer or even no chemical reagents would be introduced into the environment by the flotation treatment.

Because natural organic matter is likely to bind with the metal oxide NPs and influence their aggregation potential,[18] humic acid (HA) was thus selected as the environmentally friendly flotation-assisting reagent to be tested in the present work. HA, as one of the three organic fractions of humic-substance, is apt to interact with metal oxide NPs:[19,20] First, the large surface area of metal oxide NPs provides space for HA adsorption. Second, HA is composed of a large number of aromatic rings linked together by alkyl chains of variable lengths, resulting in a flexible skeleton that can help make bridges between TNPs or between TNP and bubble surfaces. Third, typical HA molecular structures may correspond to polyanions through the full ionization of their carboxylic groups; the positive surface charges of TNPs can be electrostatically attracted by the polyanions, resulting in the aggregation of TNP−HA. Last but not least, at acidic or neutral pH, HA looks like fibers or bundles of fibers, and these sheetlike structures may catch NPs. The strong colloidal interaction between HA and the surface of metal oxide NPs will induce HA−NP adhesion. Therefore, HA has a great potential as a flotation activator for the removal of metal NPs. Reyes-Bozo et al.[21,22] found that HA had a strong affinity with mineral species and changed the hydrophobicity of ores; therefore, it was successfully applied in their study as both flotation collector and frother for copper sulfide ores. The interaction between HA and titania NP aggregation was also studied previously:[23,24] HA could promote the aggregation as well as the flotation of TNPs. However, the related mechanisms were not completely understood and much work is still needed to further investigate the role of HA in the flotation separation of NPs. Moreover, HA is considered as a natural organic matter leading to either aesthetic issues (like unpleasant color) or undesirable health effects associated with disinfection byproducts.[25] Thereby, DAF in this study should also minimize the residual HA content in the effluent; thus, both TNPs and HA are expected to be simultaneously removed without any addition of chemical coagulants or other flotation additives.

The objective of this work was to specifically study the role of HA on the DAF separation of TNPs under different conditions. The pH effect on the flotation performance was first investigated in the absence of HA. Experiments were then carried out at various concentrations and pH values of HA solutions to evaluate the flotation efficiency. To better understand flotation mechanisms and interactions between TNPs and HA, the size and structure of aggregates were analyzed. The influence of fluid flow rates over the DAF behavior was also explored by adopting different air-to-solid ratios.

## 2. MATERIALS AND METHODS

**2.1. Chemicals.** All experiments were performed at a constant room temperature of approximately 20 °C. Deionized water with conductivity lower than 1.7 $\mu$S/cm was used to prepare the pressurized water, TNP aqueous suspensions, and all solutions. Certified analytical grade sodium hydroxide (NaOH) solution (2 mol/L, free of carbonate) (Fisher Scientific, U.K.) was diluted to 0.1 mol/L and used as pH regulator in the DAF process.

A commercial sodium salt of HA (Carl ROTH, Germany) was used for the preparation of HA stock solution with the method described previously.[23] The HA concentration was determined by TOC analyzer (Shimadzu corporation, Japan) with regard to dissolved organic carbon (DOC), and expressed as "mg/L DOC". The HA stock solution was used for 2 weeks after preparation. The effect of pH on the solubility of HA solution was tested by adding hydrochloric acid (HCl) (AR, Carl ROTH, Germany) into the prepared HA stock solution and then measuring the variation of HA concentration in the solution. It is shown in Figure 1 that the HA concentration

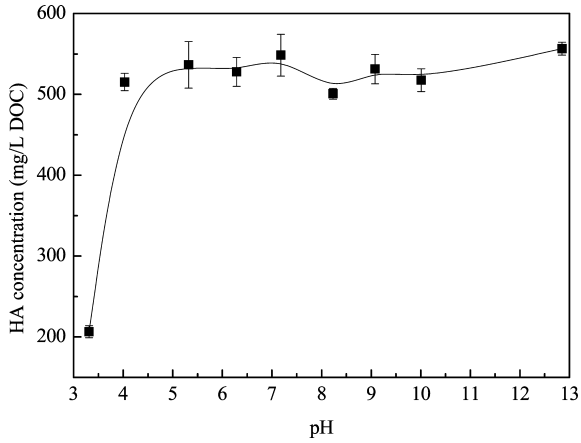


**Figure 1.** HA concentration varying with pH value of HA solution.

remained around 525 ± 25 mg/L DOC in a wide pH range of 4−13. As the pH decreased to 3.3, the HA concentration reduced to about 206.5 mg/L DOC and the resulting precipitates could be visually observed at the bottom of the vessel. This decrease of solubility as a function of pH value can be interpreted as follows: The extent of ionization of several carboxylic groups carried by HA molecules decreased significantly when pH became lower than 4 because the p$K$ of the carboxylic function is known to fall between 4.5 and 4.7. In such conditions, HA molecules exhibit weaker repulsion between one another. Owing to the presence of large hydrophobic moieties in their structure, HA molecules would thus tend to form aggregates so as to reduce the unfavorable contact with the surrounding aqueous phase, and finally sediment could even be observed. Consequently, in the

aqueous solution with a pH lower than 4, the HA molecules were not well-soluble. Other characteristics of the HA stock solution (the critical micelle concentration of HA and the relationship between DOC and dilution factor) can be found in a previous study.[23]

**2.2. TNP Aqueous Suspension.** A commercial TNP water suspension ($TiO_2$, Rutile, 5−30 nm, 15 wt %; density, 4.2 g/cm$^3$ at 20 °C) supplied by Nanostructured & Amorphous Materials Inc. (Untied States), widely applied as coating material, was chosen in this study. The influent of DAF apparatus was obtained by diluting the original suspension to 0.15 wt % with deionized water. Colloidal behaviors of TNP suspension are provided in the Supporting Information. Figure 2 shows the narrow particle size distribution of TNPs measured

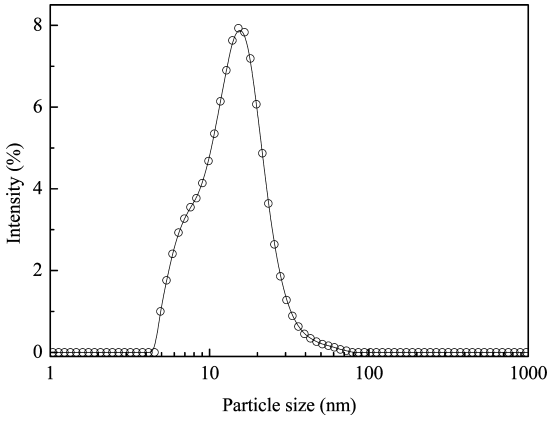


**Figure 2.** Particle size distribution of TNPs by DLS.

by dynamic light scattering (DLS, Nanotrac NPA250 from Microtrac, United States). The average particle diameter ($d_p$) was determined to be 14.5 nm. The effect of pH on zeta potential of the TNP suspension was investigated and is presented in Figure S3 of the Supporting Information. The isoelectric point (IEP) was at approximately pH 5.7. Other physicochemical properties measured and provided by the producer are summarized in Table 1.

**Table 1. Characteristics of 0.15 wt % TNP Suspension Used in DAF Experiments at about 22°C**

| item | value | item | value |
|---|---|---|---|
| turbidity (NTU) | 10.9 | Si (ppm) | ≤0.55 |
| zeta potential (mV) | +39.8 | Mg (ppm) | ≤0.45 |
| pH | 2.9 | Ca (ppm) | ≤0.60 |
| conductivity (mS/cm) | 0.701 | Pb (ppm) | ≤0.002 |

Turbidity was measured with a 2100N-IS Turbidimeter (HACH, United States); zeta potential was analyzed with a NanoZS (Malvern Instruments Ltd., U.K.); pH was measured with a pH-539 pH-meter (WTW, Germany) and a SenTix 41 pH-electrode; and conductivity was measured with a LF 538 conductivity meter (WTW, Germany) with a Tetracon 325 probe.

**2.3. DAF Experiments.** *2.3.1. DAF Apparatus and Operating Conditions.* DAF experiments were carried out in a continuous laboratory-made device (shown in Figure 3). The DAF experimental procedure has been elaborated previously.[24,26] Liquid flow rates of TNP aqueous suspension ($Q_1$), pressurized water ($Q_2$), effluent (clarified water) ($Q_3$),

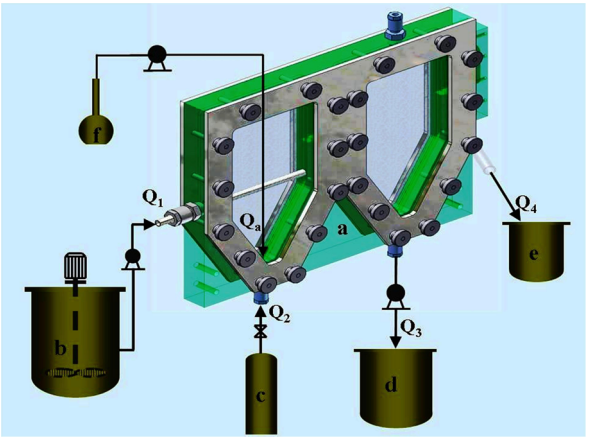


**Figure 3.** Layout of the laboratory-scale continuous DAF device: (a) flotation cell (200 × 105 × 18 mm$^3$), (b) feed tank (40 L), (c) saturation tank with pressurized water (20 L; maximum tolerated pressure, 700 kPa), (d) tank for clarified water (20 L), (e) tank for foam (5 L), and (f) flask for the additive solution (500 mL).

and reagent ($Q_a$) (NaOH or HA) were individually controlled for different operating conditions by peristaltic pumps. A pressure of 600 kPa was set in all the DAF experiments herein for the white water production. Measurements by laser diffraction sizing (Malvern Spraytec) denoted that bubbles produced with this saturator and discharge valve had an average diameter, $d_b$, of approximately 70 $\mu$m.

For the DAF application in the water engineering, a definite amount of air is necessary especially for the influent with low solid concentration; however, when the influent solids concentration increases above a certain threshold (hundreds of milligrams per liter, such as the case in the present work), the increased performance is obtained at higher mass ratios of air to solids (A/S).[27] In this study, the DAF efficiency is related to A/S due to the high concentration of TNPs, which can be expressed as

$$\mathrm{A/S} = \frac{m_{\mathrm{air}}}{m_{\mathrm{TNP}}} = \frac{\rho_{\mathrm{air}} \cdot V_{\mathrm{air}}}{\rho_{\mathrm{TNP}} \cdot V_{\mathrm{TNP}}} = \frac{\rho_{\mathrm{air}} \cdot Q_b}{\rho_{\mathrm{TNP}} \cdot Q_1 \cdot C_{0\mathrm{V}}} \quad (1)$$

where $\rho_{air}$ = 1.21 kg/m$^3$ and $\rho_{TNP}$ = 4.2 g/cm$^3$ (20 °C, 101.3 kPa). The flow rate, $Q_1$, and the volume concentration, $C_{0V}$, of the TNP aqueous suspension are predetermined; hence, the solid (TNP) flow rate, $Q_s$, can be determined by $Q_1 \cdot C_{0V}$.

The A/S is also derived from the bubble flow rate $Q_b$:

$$Q_b = K_H \cdot p \cdot Q_2 \quad (2)$$

where $K_H$ is the Henry constant (1.78 × 10$^{-4}$ L/(L·kPa), 20 °C);[28] $p$ is the relative pressure for dissolving air (600 kPa in this study). Herein, three A/S values were used in the experiments. The operating conditions for studying the effect of A/S are summarized in Table 2.

It should be noted that the ratio $Q_2/Q_1$ was determined by $K_H$, $p$, $d_b$, $d_p$, and $C_{0V}$, and the detailed calculation can be found in the Supporting Information. When the weight concentration of TNPs was fixed as 0.15%, $Q_2/Q_1$ was 559%, which should have been the minimum value but in fact would be too high for dilute suspensions in the water engineering; therefore, the values of $Q_2/Q_1$ adopted in this study were adjusted to be lower (as presented in Table 2, though they were still high).

Although the focus of the present work was on the phenomenon of TNP flotation separation and not on the

**Table 2. Operating conditions of DAF experiments**

| no. | $Q_1$ (mL/min) | $Q_s$ (mL/min) | $Q_2$ (mL/min) | $Q_2/Q_1$ (%) | $Q_b$[a] (mL/min) | $C_b$[b] (mg/L) | $Q_3$ (mL/min) | A/S |
|---|---|---|---|---|---|---|---|---|
| 1 | 70 | 0.028 | 167 | 238.6 | 17.8 | | 100 | 0.18 |
| 2 | 70 | 0.028 | 100 | 142.9 | 10.7 | 129 | 60 | 0.11 |
| 3 | 140 | 0.056 | 100 | 71.4 | 10.7 | | 100 | 0.06 |

[a]The relationship between $Q_b$ and $Q_2$ obeys Henry's Law in eq 2. [b]The bubble concentration, $C_b$, is calculated as follows: $C_b = Q_b{\cdot}\rho_{air}/Q_2 = K_H{\cdot}p{\cdot}\rho_{air}$ [$K_H = 1.78 \times 10^{-4}$ L/(L·kPa) and $\rho_{air} = 1.21$ kg/m$^3$ at 20 °C and 101.3 kPa].

optimization of the process, it should also be noted that most of the fluid exiting the DAF is directed to the foam/sludge compartment, which could negatively affect the efficiency of the system.

*2.3.2. Evaluation of DAF Performance.* Samples of clarified water were taken after 5 min of the DAF test. This duration was determined by preliminary flotation experiments which confirmed that the effluent could reach a steady state after 4.5 min. Ti contents in the effluent and influent were analyzed by inductively coupled plasma atomic emission spectroscopy (ICP-AES). Zeta potential, pH, and residual DOC concentration were also measured to characterize the water characteristics before and after DAF.

The TNP removal efficiency, $\eta$, was determined by excluding the dilution effect caused by the addition of pressurized water:

$$\eta = \left(\frac{C_D{\cdot}Q_3 - C_3{\cdot}Q_3}{C_D{\cdot}Q_3}\right) \times 100\% = \left[1 - \frac{C_3{\cdot}(Q_1 + Q_2 + Q_a)}{C_0{\cdot}Q_1}\right] \times 100\% \quad (3)$$

where $C_0$ and $C_3$ are TNP concentrations of influent and effluent, respectively. $C_D$ was considered to be the diluted TNP concentration resulting from the addition of pressurized water and reagent solution and could be calculated as follows:

$$C_D = \frac{C_0{\cdot}Q_1}{Q_1 + Q_2 + Q_a} \quad (4)$$

A similar efficiency $\eta'$ was used to estimate the amount of HA removed from the stock solution by flotation:

$$\eta' = \left(\frac{C_D'{\cdot}Q_3 - C_3'{\cdot}Q_3}{C_D'{\cdot}Q_3}\right) \times 100\% = \left[1 - \frac{C_3'{\cdot}(Q_1 + Q_2 + Q_a)}{C_{HAstock}{\cdot}Q_a}\right] \times 100\% \quad (5)$$

where $C_{HAstock}$ and $C_3'$ were HA concentrations in the HA stock solution and in the DAF effluent, respectively. $C_D'$ was the HA concentration caused by the dilution effect:

$$C_D' = \frac{C_{HAstock}{\cdot}Q_a}{Q_1 + Q_2 + Q_a} \quad (6)$$

*2.3.3. Structure and Size Measurement of TNP Aggregates in the Surface of the Separation Zone of the DAF Unit.* Flocs formed under operating conditions no. 2 (Table 2) with the following physiochemical conditions ($pH_{DAF\ suspension}$ = 5.5 for pH adjusted DAF, and HA dosages of 6.8 and 11.1 mg/L DOC for HA assisted DAF) were carefully collected by plastic Pasteur pipet from the water surface of the separating zone immediately after DAF and analyzed by a Mastersizer 2000 instrument (Malvern Instruments Ltd., U.K.).

The particle size distribution was measured via laser diffraction. The mean diameter, $d_{50}$, was selected as the representative aggregate size, though similar general trends were observed from $d_{10}$ and $d_{90}$ in all experimental conditions. The small-angle laser light scattering method was used to determine fractal dimension, $D_f$, of DAF aggregates. Particles in samples scatter light proportionally to their size, which is independent of which part of the particle at a constant angle.[29] The total scattered light intensity, $I$, is a function of the scattering vector, $Q$, which can be described as wavenumber. $Q$ is the difference between the incident and scattered wave vectors of the radiation beam in the medium given by

$$Q = \frac{4\pi n \sin(\theta/2)}{\lambda} \quad (7)$$

where $n$ is the refractive index of the suspending medium, $\theta$ the scattering angle, and $\lambda$ the wavelength of the radiation. It has been shown that for a mass fractal aggregate, which satisfies conditions for Rayleigh−Gans−Debye regime, the scattered light intensity, $I$, scales with $Q$ according to[30]

$$I \propto Q^{-D_f} \quad (8)$$

This relationship holds when the length scale of investigation is much larger than the primary particles size and much smaller than the aggregate size.[31] This condition was satisfied in the present case where the primary NP size was around 15 nm, while the floc size could be at least 10 $\mu$m.

## 3. RESULTS AND DISCUSSION

**3.1. Influence of pH on Flotation Separation of TNPs in the Absence of HA.** Studies by Dunphy Guzman et al.,[32] Pettibone et al.,[33] and French et al.[34] indicated that pH can significantly affect the stability, surface adsorption, and reactivity of TNPs in suspension. Hence, it is of great importance to investigate the effect of pH on the flotation performance before exploring the performance of HA-assisted flotation. Operating conditions no. 2 in Table 2 was used. Experiments were conducted at varying pH values from 3.2 to 9.9 by adding NaOH solution into the contact cell during the experimental process. Flow rates of NaOH ($Q_a$) were determined by required pH values.

The obtained results are depicted in Figure 4. The removal efficiency remained above 10% within the overall tested pH range. The TNP removal efficiency, $\eta$, remained low at pH < 4.5 but increased sharply at pH around 5. The highest removals (around 60%) were achieved at the pH values of 5.5 and 6.4 (63.8% and 56.5%, respectively). $\eta$ kept falling when the flotation suspension was basic. Along with the change of TNP removal, the variation of the zeta potential went through three stages: (i) being positive at around +40 mV (and even slightly increasing from pH 3.2 to 4.6), (ii) sharply dropping and showing a reversal from pH 4.6 to 8.8, and (iii) remaining at an average level of approximately −38 mV at pH greater than 8.0.

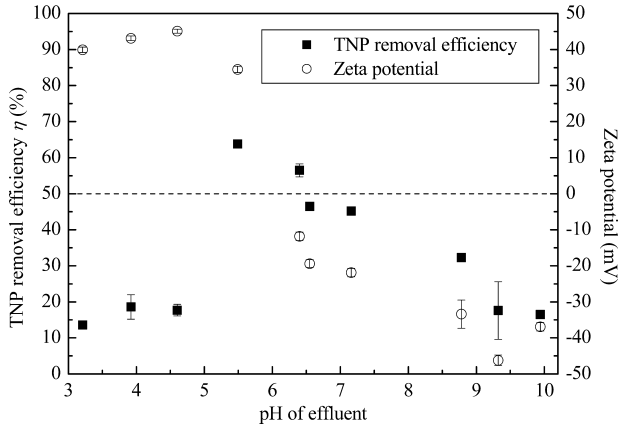


**Figure 4.** TNP removal efficiency and zeta potential versus pH of effluent.

The results may be interpreted by invoking the charging behavior of metal oxides, which is intimately related to the difference between the pH of the contacting solution, and the IEP of solid particles. $TiO_2$ is known to present numerous −OH surface groups that are able to favorably create hydrogen bonds with water molecules.[34] When pH < IEP, $TiO_2 - OH + H_3O^+ \Rightarrow TiO_2 - OH_2^+ + H_2O$, surfaces are then positively charged; when pH > IEP, $TiO_2 - OH + OH^- \Rightarrow TiO_2 - O^- + H_2O$, surfaces are then negatively charged. When the pH of solution gets close to the IEP, $TiO_2 - OH_2^+ + OH^- \Rightarrow TiO_2 - OH + H_2O$, surfaces are near neutral. In this study, the IEP occurring at around pH 6.1 was just in stage ii where about 60% of the TNPs could be removed, pointing out that the addition of $OH^-$ destabilized the positively charged TNPs by neutralizing the surface charges: when there was no more electrostatic repulsion between TNPs (the pH of suspension was close to IEP), the aggregation of TNPs was significantly promoted and the resulting large aggregates were thus more easily captured by bubbles.

It should be pointed out that the maximum TNP removal was only ∼64% by just adjusting the pH of initial TNP suspension; other flotation-assisting reagents, such as HA, were therefore required in order to enhance the DAF performance.

**3.2. HA-Assisted Flotation for the Removal of TNPs.** *3.2.1. Effect of HA Concentration.* The influence of HA on the DAF performance (TNP separation efficiency, HA removal, zeta potential, and pH of flotation effluent) was studied under the same operating conditions as in section 3.1. The HA dosage ranging from 0 to 21 mg/L DOC was controlled by changing the flow rate of the HA stock solution. Because pH greatly influenced the flotation efficiency according to the experimental results of section 3.1, the HA stock solutions were adjusted to pH 4.7, 6.2, 8.9, and 12.1 before being added into the flotation aqueous system.

As described in Figure 5, when $pH_{HAstock}$ was 4.7, a TNP removal efficiency better than 92.0% was achievable at HA dosages greater than 11.1 mg/L DOC. With a maximum TNP separation of 99.6%, using about 20.8 mg/L DOC of HA, as much as 94.2% of HA was simultaneously removed; meanwhile, the zeta potential of flotation aggregates was −14.5 mV, and the pH of flotation suspension was around 3.6. Increasing the pH of HA stock solution to 6.2, DAF then removed around 99.0%

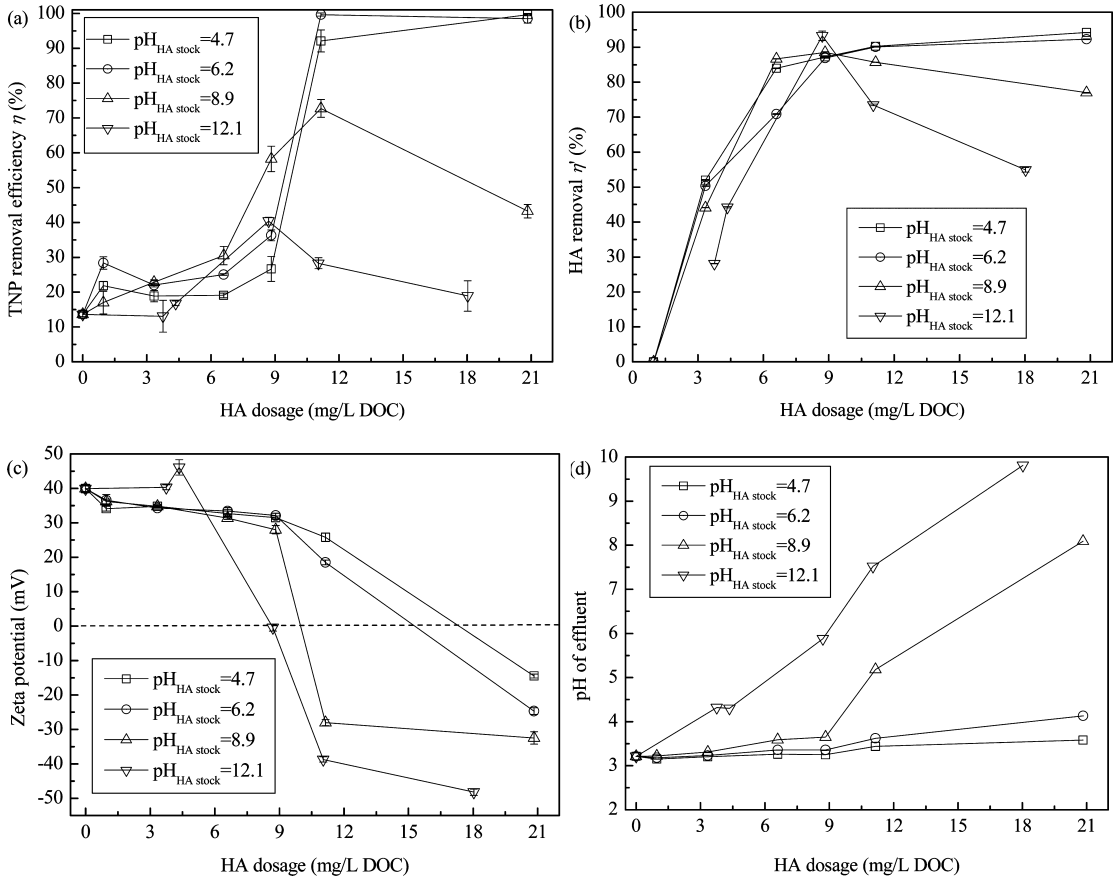


**Figure 5.** Flotation behavior as a function of HA dosage (a) TNP removal efficiency, (b) HA removal, (c) zeta potential, and (d) pH of effluent.

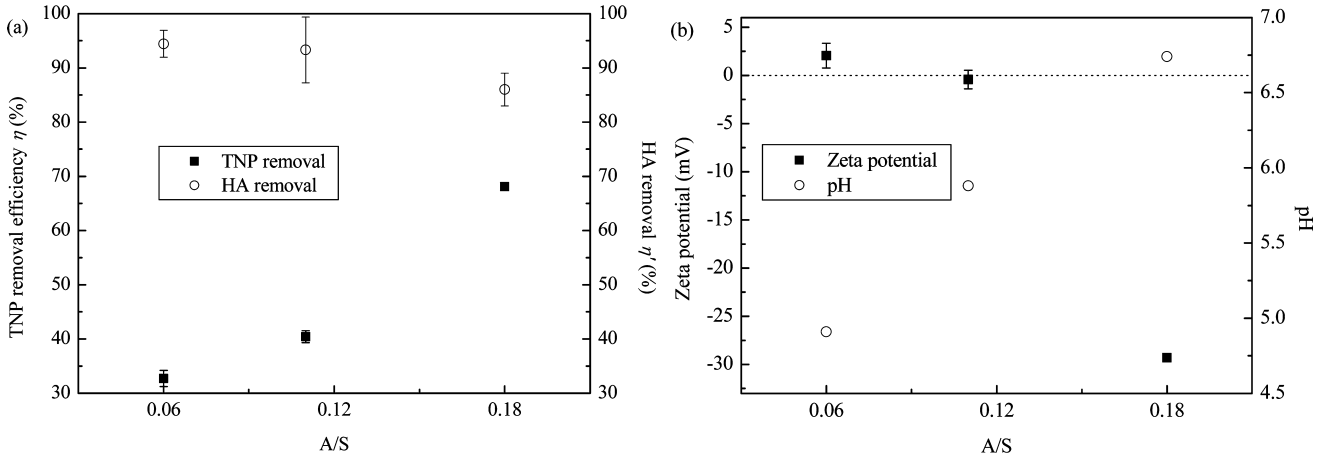


**Figure 6.** Comparison of flotation performances at different A/S ratios: (a) TNP and HA removals and (b) zeta potential and pH of effluent.

and 91.0% of TNPs and HA, respectively, by dosing more than 11 mg/L DOC of HA. Under these conditions, the zeta potential declined to −24.7 mV and the pH rose to 4.1. When $pH_{HA\ stock}$ was further increased to the basic range (8.9 and 12.1), the maximum TNP removals fell to 72.7% ($pH_{HA\ stock}$ = 8.9, HA dosage = 11.1 mg/L DOC) and then to 40.4% ($pH_{HA\ stock}$ = 12.1, HA dosage = 8.7 mg/L DOC); HA removals were 85.7% and 93.3%, respectively. The pH value of effluents turned from acidic to basic with the increasing dosage of HA, owing to the addition of alkaline HA stock solutions. Similarly to what was observed from the pH-induced flotation in section 3.1, when the zeta potential was around zero, the flotation suspension exhibited the lowest stability; thus, the TNP aggregation was facilitated.[23,35] As for the effects of operating conditions on the HA-assisted DAF for the TNP removal, the related exploration will be carried out in the following part.

*3.2.2. Effect of A/S Ratio.* The parameter of A/S is closely related to flow rates of bubbles and influent, as well as to the influent concentration; hence, it significantly influences the separation efficiency of flotation. Three A/S values (0.06, 0.11, and 0.18 in Table 2) were tested. The pH of the HA stock solution was chosen to be 12.1 to allow the probable increase of flotation efficiency with A/S (the TNP removal at $pH_{HA\ stock}$ = 12.1 in section 3.2.1 was low in comparison with those at lower pH values). The DAF performance as a function of HA dosage at each A/S is presented in Figures S6−S9, indicating that (1) the use of DAF-assisting reagents was necessary because the TNP removal efficiencies were as low as 4.5%, 13.6% and 17.7%, respectively, without the HA addition and (2) the optimum HA concentrations for these three A/S values (0.06, 0.11, and 0.18) were 11.8, 8.7, and 6.8 mg/L DOC, respectively. The specific comparison was made among different A/S ratios at the optimum HA dosages in Figure 6.

For the A/S ratio of 0.06 and 0.11, the pH values of the flotation system were 4.9 and 5.8, respectively, and the related zeta potentials approached zero. Although the electrostatic attraction between TNPs and basic HA could result in the TNP−HA aggregates by the heterocoagulation, the insufficient air bubbles hardly supported a high TNP removal. It is worth noting that the TNP removal efficiency increased from ∼40.4% (A/S = 0.11) to ∼68.1% (A/S = 0.18). With the higher air input (A/S = 0.18), a greater TNP removal could then be obtained because more air bubbles were introduced into the DAF system, giving rise to a greater bubble surface area available for collecting TNPs.

**3.3. Size Distribution and Structural Characteristics of Aggregates in the Surface of the Separation Zone of the DAF Unit.** The aggregate (particle) size affects the collision efficiency in the flotation process and hence may influence the removal efficiency. As presented in Figure 7, the addition of HA

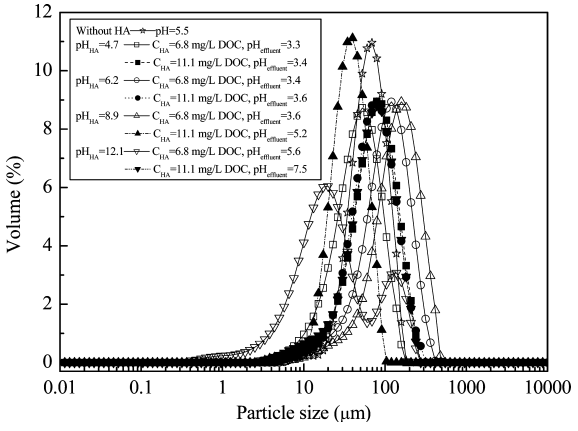


**Figure 7.** Aggregate size distribution under different conditions.

or $OH^-$ ions resulted in the formation of large TNP aggregates, with $d_p$ varying from 19 to 136 μm. Because the recovery of particles by flotation was confirmed to be the most successful at the particle size between 10 and 200 μm,[11−13] the flotation-assisting reagents (HA or pH regulator) used here could facilitate the TNP removal.

Fractal structure is among the crucial physical properties having an impact on the efficiency of unit processes in water treatment works.[36] TNP aggregates in the presence and absence of HA generated in the DAF process were compared in terms of fractal dimension, $D_f$ (Figure 8). The relationship between the scattered light intensity ($I$) and wavenumber ($Q$) (eq 8) on a log−log scale for the $D_f$ determination is given in Figure 8a. All the $D_f$ values were restricted to the same $Q$ range. For all the $D_f$ calculations, the determination coefficient of the regression line was high ($R^2$ > 0.99). As shown, the flotation flocs under investigation exhibited the typically scattering behavior of mass fractal objects. The $D_f$ values were in the range of 1.80−2.90. It could be observed that the greater addition of HA molecules during flotation could bring about more compact flocs, which was possibly caused by the tight combination between TNPs and the sufficient HA. From a combined view of

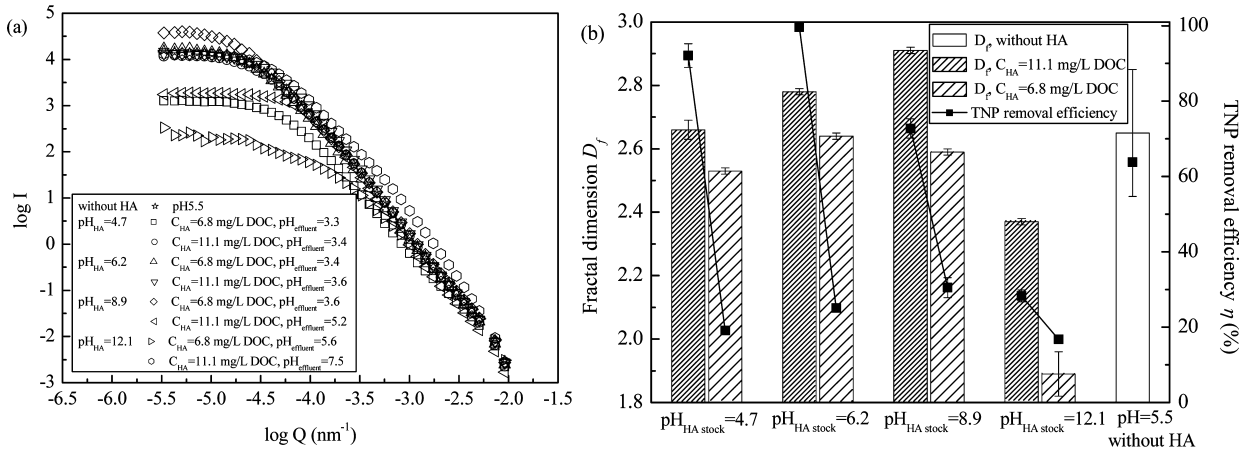


**Figure 8.** (a) Static light-scattering plots of flotation flocs formed in different physiochemical conditions of DAF; (b) comparison of fractal dimension values of flotation aggregates under different conditions.

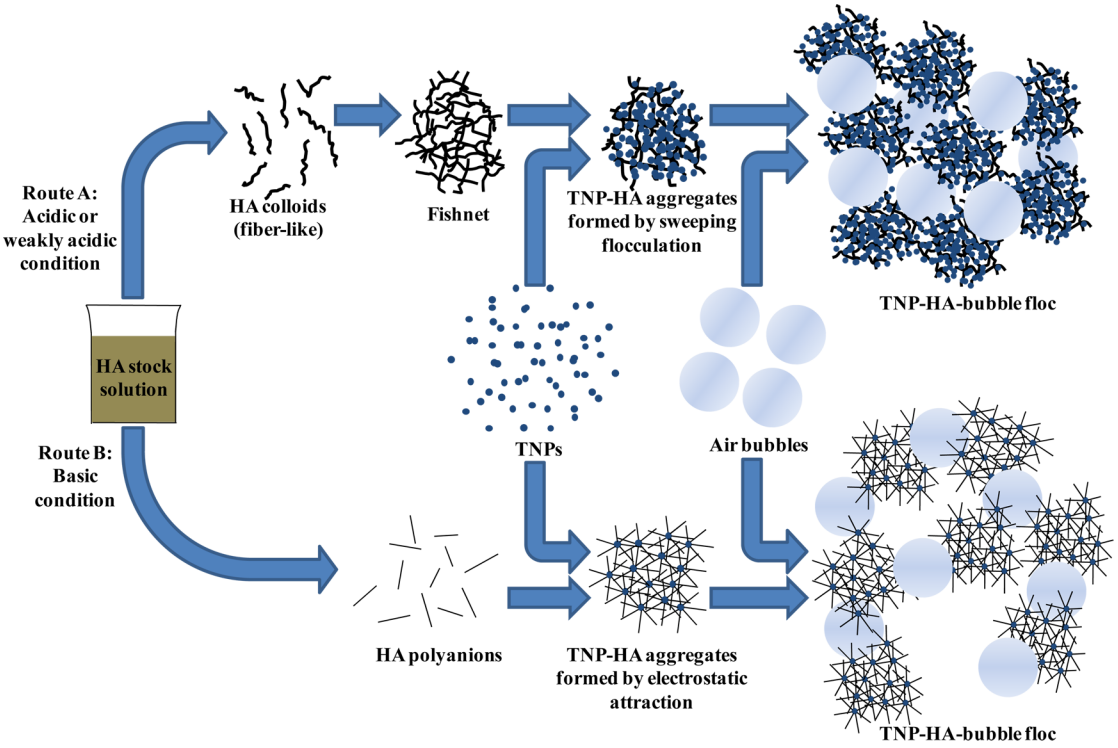


**Figure 9.** Proposed interfacial mechanisms of floc formation in the HA-enhanced DAF for TNP removal.

particle removal and floc structural character, the flocs with close conformation rather than the open structure gave more benefit in DAF under the same flotation conditions.

**3.4. Mechanism Discussion of HA-Involved DAF.** It is obvious in section 3.2.1 that the acidic HA stock solution helped to enhance the TNP removal by DAF. The optimum flotation efficiency was obtained when the pH values of the effluents were lower than 4 (Figure 5d). The possible interfacial process could be illustrated as route A in Figure 9. Being in the acidic or weakly acidic solutions, the majority of HA were not well-soluble (shown in Figure 1). Owing to the presence of their large hydrophobic moieties, the HA molecules possibly tend to aggregate in order to escape from the surrounding aqueous environment. They may be organized as fibers or as bundles of fibers at acidic or neutral pH.[19] Thus, an extended colloidal fishnet is created, in which the TNPs are enmeshed or trapped by sweeping flocculation, allowing also an easy bubble capture in DAF. This effect was notably reinforced with a greater amount of HA molecules. Accordingly, high HA removals were effective because the majority of HA molecules should be implicated in these consolidated particle aggregates which were collected and removed by DAF bubbles.

In the basic HA stock solutions (i.e., at pH 8.9 and 12.1), when the pH values of the effluents were lower than the IEP of TNPs, the HA molecules might directly adsorb onto the positively surface-charged TNPs through electrostatic attraction or via ligand exchange with their phenolic (−OH) and/or carboxylic (−COOH) groups.[20,23] The particle aggregation was thereby promoted as elaborated by route B in Figure 9. It was in accordance with Figure 5a,c (with these alkaline HA stock solutions) that high TNP removal efficiencies were attained at the point where the zeta potential was reversed. However, when

the pH became greater than IEP, the negatively surface-charged TNPs were electrostatically repulsed by the HA polyanions in the bulk, in which case the decrease of TNP removal efficiency was observed. A large number of HA molecules were collected and removed probably through the adhesion of the accessible hydrophobic portions of HA polyanions onto the air bubbles. Nevertheless, this bubble−HA attachment apparently decreased when the pH of the flotation system was >6, suggesting that the repulsion between the fully ionized HA polyanions and the negatively charged bubbles[31,33] was strong enough to hinder their adhesion.

In addition, the difference in floc morphology is also presented in Figure 9. As a direct comparison, TNPs were found to compactly aggregate with the HA colloids or the fiberlike HA molecules (in the acidic solution) and the weakly hydrolytic HA (in the basic solution) in flotation ($D_f$ > 2.50 in Figure 8); however, the HA polyanions in the highly basic solution were apt to form loose flocs with TNPs due to their expanded structures.

Encouragingly and interestingly, favorable HA removals were obtained at comparatively wide HA dosages and all the tested A/S ratios. This demonstrated the participation of HA in the DAF process. This was in agreement with a previous study which highlighted the importance of the strong interaction between TNPs and HA molecules via the analyses of Fourier transform infrared spectrum (FT-IR), aggregate size distribution, and HA adsorption on TNPs.[23] Herein, the TNP removal by DAF was deeper investigated and analyzed by particularly changing the HA properties in flotation, finally determining the flotation characteristics with the assistance of HA but in the absence of traditional chemical coagulants.

## 4. CONCLUSIONS

In the present study, the HA-assisted DAF was found to efficiently enhance the TNP removal in a coagulant-free process when the HA property was well-controlled. The pH value of the flotation suspension greatly impacted the TNP removal efficiency because the positive surface charges of TNPs could be effectively neutralized by $OH^-$ through electrostatic attraction. In the pH-dependent DAF, the highest TNP removal of 63.8% was obtained near the IEP of TNPs. As for the HA-involved DAF, as high as 99.0% of TNPs and more than 90.0% of HA were simultaneously removed when the HA stock solutions were adjusted to be acidic. In those cases, the HA molecules were poorly soluble in the flotation suspension; thus, the presence of those extended HA aggregates and fiberlike HA molecules in the acidic or neutral suspension might act as a colloidal fishnet in which TNPs could be enmeshed or trapped. Consequently, the bubble capture efficiency in DAF was reinforced. In terms of the characteristics of aggregates in flotation, the size of TNP−HA flocs fell in the particle range where aggregates could be efficiently captured by bubbles, and the flotation separation was then facilitated. Those flocs with denser conformation were preferable in DAF. Moreover, it was shown that a higher A/S ratio could help to improve the DAF efficiency by providing a greater bubble interface area. In sum, with respect to the high TNP removal efficiency and the low chemical reagent addition, using HA as DAF activator was obviously a sound choice because the chemical coagulants were not needed and the extra DOC pollution was not generated. However, it should also be pointed out that a large amount of pressurized water was still demanded in the current DAF process. In future research, several possible and interesting aspects may be particularly focused on: (1) simultaneously removing NPs and HA by DAF through just preadjusting the pH of the HA-contained natural water to an acidic value; (2) improving the experimental design and the DAF apparatus, reducing the amount of pressurized water used, and controlling the amount of foam/sludge produced in that process; and (3) neutralizing the pH before the final discharge when the effluent is acidic.

## AUTHOR INFORMATION


### Corresponding Author

*Tel: +33 (0)5 61 55 96 86. Fax: +33 (0)5 61 55 97 60. E-mail: pascal.guiraud@insa-toulouse.fr.

### ORCID

Ming Zhang: 0000-0002-4878-5420

### Present Address

§M.Z.: State Key Laboratory of Pollution Control and Resources Reuse, Key Laboratory of Yangtze River Water Environment, Institute of Biofilm Technology, College of Environmental Science and Engineering, Tongji University, 1239 Siping Road, Shanghai 200092, PR China.


### Notes

The authors declare no competing financial interest.

## ACKNOWLEDGMENTS


This study was completed with the assistance of Marie-Line de Solan Bethmale and Mallorie Tourbin at the Laboratoire de Génie Chimique (LGC) of Toulouse University for the ICP-AES measurement. The authors also acknowledge China Scholarship Council (CSC) for the scholarship.


## REFERENCES


(1) Robichaud, C. O.; Uyar, A. E.; Darby, M. R.; Zucker, L. G.; Wiesner, M. R. Estimates of Upper Bounds and Trends in Nano-$TiO_2$ Production as a Basis for Exposure Assessment. *Environ. Sci. Technol.* **2009**, *43*, 4227.

(2) Moore, M. N. Do Nanoparticles Present Ecotoxicological Risks for the Health of the Aquatic Environment? *Environ. Int.* **2006**, *32*, 967.

(3) Wiesner, M. R.; Lowry, G. V.; Alvarez, P.; Dionysiou, D.; Biswas, P. Assessing the Risks of Manufactured Nanomaterials. *Environ. Sci. Technol.* **2006**, *40*, 4336.

(4) Sayes, C. M.; Wahi, R.; Kurian, P. A.; Liu, Y.; West, J. L.; Ausman, K. D.; Warheit, D. B.; Colvin, V. L. Correlating Nanoscale Titania Structure with Toxicity: A Cytotoxicity and Inflammatory Response Study with Human Dermal Fibroblasts and Human Lung Epithelial Cells. *Toxicol. Sci.* **2006**, *92*, 174.

(5) Dröge, W. Free Radicals in the Physiological Control of Cell Function. *Physiol. Rev.* **2002**, *82*, 47.

(6) Wang, J.; Zhou, G.; Chen, C.; Yu, H.; Wang, T.; Ma, Y.; Jia, G.; Gao, Y.; Li, B.; Sun, J.; Li, Y.; Jiao, F.; Zhao, Y.; Chai, Z. Acute Toxicity and Biodistribution of Different Sized Titanium Dioxide Particles in Mice after Oral Administration. *Toxicol. Lett.* **2007**, *168*, 176.

(7) Thanh, L. H. V.; Liu, J.-C. Flotation Separation of Soluble and Colloidal Indium from Aqueous Solution. *Ind. Eng. Chem. Res.* **2014**, *53*, 1242.
(8) George, P.; Nguyen, A. V.; Jameson, G. J. Assessment of True Flotation and Entrainment in the Flotation of Submicron Particles by Fine Bubbles. *Miner. Eng.* **2004**, *17*, 847.
(9) Ralston, J.; Fornasiero, D.; Hayes, R. Bubble−particle Attachment and Detachment in Flotation. *Int. J. Miner. Process.* **1999**, *56*, 133.
(10) Ralston, J.; Dukhin, S. S.; Mishchuk, N. A. Wetting Film Stability and Flotation Kinetics. *Adv. Colloid Interface Sci.* **2002**, *95*, 145.
(11) Reay, D.; Ratcliff, G. A. Removal of Fine Particles from Water by Dispersed Air Flotation: Effects of Bubble Size and Particle Size on Collection Efficiency. *Can. J. Chem. Eng.* **1973**, *51*, 178.
(12) Nguyen, A. V.; George, P.; Jameson, G. J. Demonstration of a Minimum in the Recovery of Nanoparticles by Flotation: Theory and Experiment. *Chem. Eng. Sci.* **2006**, *61*, 2494.
(13) Miettinen, T.; Ralston, J.; Fornasiero, D. The Limits of Fine Particle Flotation. *Miner. Eng.* **2010**, *23*, 420.
(14) Edzwald, J. K. Dissolved Air Flotation and Me. *Water Res.* **2010**, *44*, 2077.
(15) Liu, Y.; Tourbin, M.; Lachaize, S.; Guiraud, P. Silica Nanoparticle Separation from Water by Aggregation with $AlCl_3$. *Ind. Eng. Chem. Res.* **2012**, *51*, 1853.
(16) Lien, C. Y.; Liu, J. C. Treatment of Polishing Wastewater from Semiconductor Manufacturer by Dispersed Air Flotation. *J. Environ. Eng.* **2006**, *132*, 51.
(17) Liu, Y.; Tourbin, M.; Lachaize, S.; Guiraud, P. Flotation Separation of $SiO_2$ Nanoparticles from Water. IWA Conference Flotation, Columbia University, New York, October 29−November 1, 2012.
(18) Ma, Z.; Yin, X.; Ji, X.; Yue, J.; Zhang, L.; Qin, J.; Valiyaveettil, S.; Adin, A. Evaluation and Removal of Emerging Nanoparticle Contaminants in Water Treatment: A Review. *Desalin. Water Treat.* **2016**, *57*, 11221.
(19) Xie, L.; Shang, C. Role of Humic Acid and Quinone Model Compounds in Bromate Reduction by Zerovalent Iron. *Environ. Sci. Technol.* **2005**, *39*, 1092.
(20) Yang, K.; Lin, D.; Xing, B. Interactions of Humic Acid with Nanosized Inorganic Oxides. *Langmuir* **2009**, *25*, 3571.
(21) Reyes-Bozo, L.; Herrera-Urbina, R.; Escudey, M.; Godoy-Faúndez, A.; Sáez-Navarrete, C.; Herrera, M.; Ginocchio, R. Role of Biosolids on Hydrophobic Properties of Sulfide Ores. *Int. J. Miner. Process.* **2011**, *100*, 124.
(22) Reyes-Bozo, L.; Herrera-Urbina, R.; Sáez-Navarrete, C.; Otero, A. F.; Godoy-Faúndez, A.; Ginocchio, R. Rougher Flotation of Copper Sulphide Ore Using Biosolids and Humic Acids. *Miner. Eng.* **2011**, *24*, 1603.
(23) Zhang, M.; Guiraud, P. Elimination of $TiO_2$ Nanoparticles with the Assist of Humic Acid: Influence of Agglomeration in the Dissolved Air Flotation Process. *J. Hazard. Mater.* **2013**, *260*, 122.
(24) Zhang, M. *Elimination de Nanoparticules par des Procédés de Flottation*; PhD thesis, Institut National des Sciences Appliquées: Toulouse, France, 2015.
(25) Xue, N.; Wang, X.; Zhang, F.; Wang, Y.; Chu, Y.; Zheng, Y. Effect of $SiO_2$ Nanoparticles on the Removal of Natural Organic Matter (NOM) by Coagulation. *Environ. Sci. Pollut. Res.* **2016**, *23*, 11835.
(26) Liu, Y. *Elimination de Nanoparticules d'Effluents Liquides*; PhD thesis, Institut National des Sciences Appliquées: Toulouse, France, 2010.
(27) Wang, L.; Fahey, E.; Wu, Z. Dissolved Air Flotation. In *Physicochemical Treatment Processes, Handbook of Environmental Engineering*; Wang, L., Hung, Y.-T., Shammas, N., Eds.; Humana Press: Totowa, NJ, 2005, 431.
(28) Blazy, P.; Jdid, E. A. Flottation: Aspects Pratiques. *Tech. Ing., Génie des Procédés* **2000**, *J3*, J3360.
(29) Jarvis, P.; Jefferson, B.; Parsons, S. A. Breakage, Regrowth, and Fractal Nature of Natural Organic Matter Flocs. *Environ. Sci. Technol.* **2005**, *39*, 2307.
(30) Bushell, G. C.; Yan, Y. D.; Woodfield, D.; Raper, J.; Amal, R. On Techniques for the Measurement of the Mass Fractal Dimension of Aggregates. *Adv. Colloid Interface Sci.* **2002**, *95*, 1.
(31) Guan, J.; Waite, T. D.; Amal, R. Rapid Structure Characterization of Bacterial Aggregates. *Environ. Sci. Technol.* **1998**, *32*, 3735.
(32) Dunphy Guzman, K. A.; Finnegan, M. P.; Banfield, J. F. Influence of Surface Potential on Aggregation and Transport of Titania Nanoparticles. *Environ. Sci. Technol.* **2006**, *40*, 7688.
(33) Pettibone, J. M.; Cwiertny, D. M.; Scherer, M.; Grassian, V. H. Adsorption of Organic Acids on $TiO_2$ Nanoparticles: Effects of pH, Nanoparticle Size, and Nanoparticle Aggregation. *Langmuir* **2008**, *24*, 6659.
(34) French, R. A.; Jacobson, A. R.; Kim, B.; Isley, S. L.; Penn, R. L.; Baveye, P. C. Influence of Ionic Strength, pH, and Cation Valence on Aggregation Kinetics of Titanium Dioxide Nanoparticles. *Environ. Sci. Technol.* **2009**, *43*, 1354.
(35) Simate, G. S.; Iyuke, S. E.; Ndlovu, S.; Heydenrych, M. The Heterogeneous Coagulation and Flocculation of Brewery Wastewater Using Carbon Nanotubes. *Water Res.* **2012**, *46*, 1185.
(36) Chau, K. W. Investigation on Effects of Aggregate Structure in Water and Wastewater Treatment. *Water Sci. Technol.* **2004**, *50*, 119.